

# Optimization of Finocyl Grain Geometries of Solid Rocket Boosters

G. Poppe<sup>†,1</sup>, P. Koch<sup>2</sup>, O. Božić<sup>3</sup> and D. Lancelle<sup>4</sup>

German Aerospace Center (DLR), Institute of Aerodynamics and Flow Technology (AS),

Lilienthalplatz 7, D-38108 Braunschweig, Germany

<sup>1</sup>georg.poppe@dlr.de    <sup>2</sup>patrick.koch85@gmail.com

<sup>3</sup>ognjan.bozic@dlr.de    <sup>4</sup>d.m.lancelle@googlemail.com

<sup>†</sup>Corresponding author

## Abstract

A common propellant grain geometry for solid rocket motors consisting of a combined cylindrical and finocyl geometry is explained. The burn-off is simulated by a DLR simulation tool, which gives amongst others a thrust curve as the result. The burn-off simulator was coupled with an optimizer, which uses a Mesh Adaptive Direct Search method to find an optimal solution using a black box program. The assessment function and several constraints are explained. A propellant grain for a possible booster stage for a hypothetical space launcher is designed using the combination of the burn-off simulator and the optimizer. The combination of both tools produces sufficient results for the predesign phase of a solid rocket motor.

**Keywords** propellant grain, solid rocket motor, optimization, burn-off simulation, european space launcher

## Abbreviations

AHRES	Advanced Hybrid Rocket Engine Simulation
CEA	Chemical Equilibrium with Applications
HTPB1912	Propellant mixture of 69% Ammonium Perchlorate (NH <sub>4</sub> ClO <sub>4</sub> ), 12% Hydroxyl-terminated Polybutadiene (HTPB) and 19% Aluminium
LH	Latin-Hypercube sampling
MADS	Mesh Adaptive Direct Search algorithm
NOMAD	Nonlinear Optimization by Mesh Adaptive Direct Search
SRM	Solid Rocket Motor
VNS	Variable Neighborhood Search

## Nomenclature

$f$	fin radius	$E$	exponent for thrust difference
$l$	length of fin	$F$	thrust
$l_i$	length coordinate of the cylindrical geometry	$M$	total number of time steps
$o$	objective value (assessment value, constraint value)	$N$	number of fins
$r$	inner radius of the finocyl geometry	$P$	perimeter
$r_i$	radius coordinate of the cylindrical geometry	$R$	chamber radius
$t$	time	$W$	maximum web thickness
$w$	minimum web thickness	$\Delta l_i$	change of the length coordinate during the burn-off
$y$	burn distance	$\Delta r_i$	change of the radius coordinate during the burn-off
$A$	multiplier for thrust difference	$\Delta L_i$	differential length coordinate of the cylindrical geometry

## 1. Introduction

The geometry of a solid rocket motor (SRM) propellant grain is the most decisive parameter for the performance of the motor. In modern motors finocyl geometries are widely used as they provide a high thrust directly after ignition.

The design of such geometries is complex because many geometric parameters can be varied. To solve this problem a burn-off simulation tool was developed in the frame of the DLR AHRES (Advanced Hybrid Rocket Engine Simulation) program and coupled with an optimizer.

In this paper the model structure of propellant grains with a finocyl geometry is explained. The DLR burn-off simulation tool is then used to calculate the burn-off at different time steps. It uses a given geometry and the properties of the propellant. The results consist of the progress of the burning surface, the pressure, the regression rate and the thrust. The crucial problem is the combination of the finocyl and the cylindrical parts of the grain. While the burn-off in the cylindrical part is radially symmetric, the finocyl part has fins, where the burn-off has to be simulated in a different way. One problem is to simulate the burning progress at the transition zones between the cylindrical and finocyl geometries. It was solved using an approximation.

The burn-off simulation tool was coupled with the black box optimizer NOMAD (Nonlinear Optimization by Mesh Adaptive Direct Search) to find optimized finocyl geometries for a desired thrust curve. For selected input parameters one representative configuration using the developed tools is designed and analyzed. The presented solid rocket motor can be applied as predesign solution for a future European space launcher program.

## 2. Description of the general propellant grain geometry

The propellant grain consists of multiple cylindrical or conic parts and the finocyl geometry. For testing purposes it was decided to consider 11 parts, which results in 12 coordinate tuples (radius  $r_i$  and length  $l_i$ ) as illustrated in Fig. 1. The length coordinates are substituted by differential length coordinates  $\Delta L_i = l_i - l_{i-1}$  to prevent impossible coordinate combinations (e.g.  $l_i < l_{i-1}$ ) during the optimization. The part with the biggest radius is substituted with the finocyl geometry.

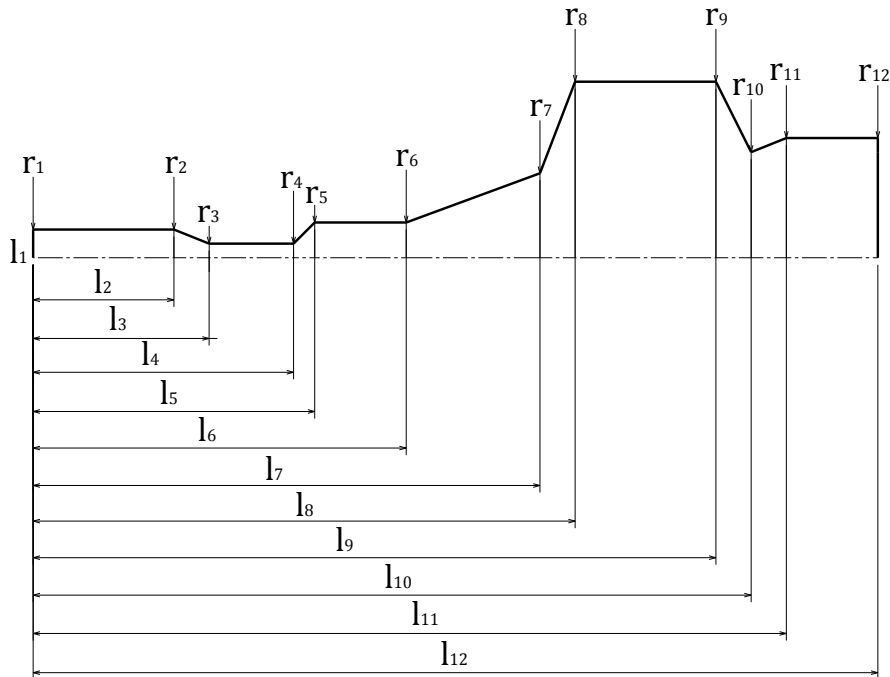


Figure 1: Basic cylinder geometry [6].

### 2.1 Finocyl geometry

The finocyl geometry (fin on cylinder) is a commonly used element in solid rocket motors to increase the burning surface. Subsequently the mass flow and the thrust level are raised. During the burn the surface area decreases significantly faster than the cylindrical part which results in a thrust peak during the first seconds. Especially for first stage boosters such a thrust curve is preferred to get off the ground with minimized gravitational losses [4].

A sketch of the geometry can be seen in Fig. 2. The finocyl geometry can be completely described by the following six parameters:

- number of fins  $N$
- minimum web thickness  $w$
- maximum web thickness  $W$
- inner radius  $r$
- fin radius  $f$
- length of fin  $l$

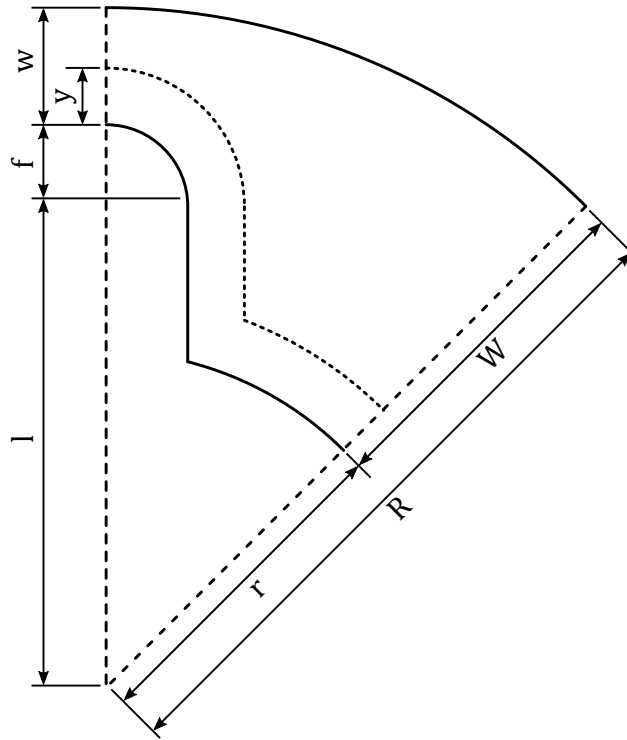


Figure 2: Finocyl geometry.

The sums of the minimal web thickness, the fin radius and the length of fin and accordingly the maximal web thickness and the inner radius add up to the chamber radius  $R$ .

$$R = w + f + l = r + W \quad (1)$$

Taking this equation into account, the number of independent parameters results to 5, which are  $N$ ,  $w$ ,  $f$ ,  $W$  and  $R$ . The sketch in Fig. 2 is then mirrored and replicated  $N$ -times to create the full finocyl geometry. The inner perimeter  $P$  can be calculated by the following formula (2) [9].

$$P_0 = 2N \left[ \frac{\pi f}{2} + \left( l - \sqrt{r^2 - f^2} \right) + r \left( \frac{\pi}{N} - \arcsin \left( \frac{f}{r} \right) \right) \right] \quad (2)$$

The burn-off of the finocyl geometry consists of two phases, which are characterized by the burn distance  $y$ . The first phase happens until the flame front reaches the casing ( $y \leq w$ ). During this phase the perimeter is determined by formula (3) [9].

$$P_1(y) = 2N \left[ \frac{\pi(f+y)}{2} + \left( l - \sqrt{(r^2 - f^2) + 2y(r-f)} \right) + (r+y) \cdot \left( \frac{\pi}{N} - \arcsin \left( \frac{f}{r} \right) \right) \right] \quad (3)$$

Phase 2 begins after the flame front has reached the casing . The perimeter is now calculated by formula (4) [9].

$$P_2(y) = 2N \left[ (f + y) \cdot \left( \alpha - \frac{\pi}{2} \right) + \left( l - \sqrt{(r^2 - f^2) + 2y(r - f)} \right) + (r + y) \cdot \left( \frac{\pi}{N} - \arcsin \left( \frac{f}{r} \right) \right) \right] \quad (4)$$

$$\text{with } \alpha = \arccos \left[ \frac{(l^2 + (f + y)^2) - R^2}{2l(f + y)} \right] \quad (5)$$

With the known perimeter the burning area can be easily calculated. The given finocyl geometry is then put into the place of the largest radius of the cylindrical geometry. The radii there are set to the minimum web thickness (here  $r_8 = r_9 = R - w$ ), which is important for the transition zones.

## 2.2 Cylindrical geometry

As illustrated in Fig. 1 the cylindrical geometry is given by 12 coordinate tuples consisting of the radius and the length. During the burn the radii and the lengths are changing. The changes can be determined by the following two formulas.

$$\Delta l_i(y) = y \cdot \sin(\alpha_i) + y \cdot \tan \left( \frac{\alpha_{i+1} - \alpha_i}{2} \right) \cdot \cos(\alpha_i) \quad (6)$$

$$\Delta r_i(y) = \sqrt{\left[ y \cdot \tan \left( \frac{\alpha_{i+1} - \alpha_i}{2} \right) \right]^2 + y^2 - \Delta l_i(y)^2} \quad (7)$$

$$\text{with } \alpha_i = \arctan \left( \frac{r_{i+1} - r_i}{l_{i+1} - l_i} \right) \quad (8)$$

After the elimination of resulting overlaps, the coordinates are trimmed to the chamber wall coordinates. While convex corners persist to be sharp corners during the burn-off, concave corners are rounded. Currently the rounding effect is not yet implemented, which leads to a negligible error during the burn-off calculation.

## 2.3 Transition zone of cylindrical and finocyl geometries

The transition zone (see Fig. 3) between the cylindrical and the finocyl geometry is complicated to describe with analytical formulas. During the burn the fins are disappearing faster than the conic part beneath. At the moment the surface area is approximated by a conus with the perimeters of the cylindrical and the finocyl part.

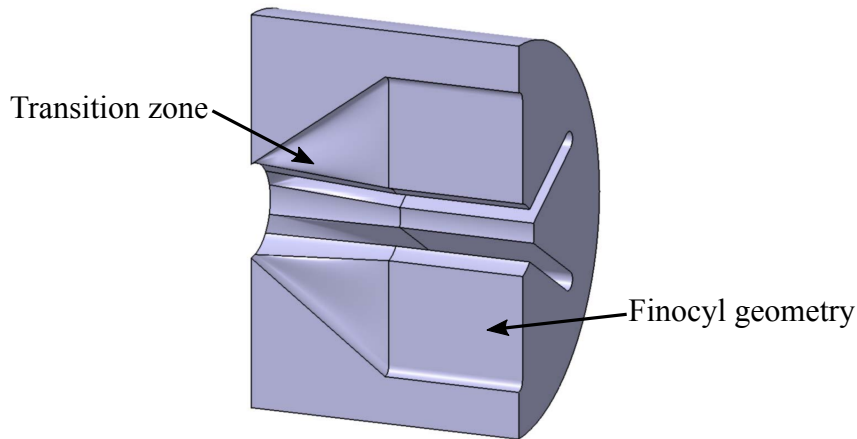


Figure 3: CAD section model of the transition zone between the cylindrical and finocyl geometry [6]

## 3. Optimization

The NOMAD optimizer was used to derive the geometry, which delivers a thrust curve equal or quite similar with the desired thrust curve defined in the requirements. NOMAD is open-source and the algorithm is well documented [1, 7]. The optimizer uses a black box program, which returns the result of an assessment function. The target of NOMAD is to minimize this result. In this case the described burn-off simulator is the black box program. The value of the

assessment function is the result of the comparison between the desired and the calculated thrust curve. To only consider results, which fulfill a certain condition, multiple constraints can be defined. The values of the constraints are reduced to zero. Once the constraint is fulfilled only black box results which comply with the condition are accepted. During the optimization of the propellant grain the burn time difference between desired and calculated was used as constraint.

The optimizer uses the so-called "Mesh Adaptive Direct Search" (MADS) algorithm to search for the input parameters. It creates a multidimensional discretized mesh of the input variables inside the given boundaries. The intersections of the mesh represent sets of values which can be used as solver input parameters. During each iteration a search step and a poll step are performed. At the beginning a search step is conducted. During this step the next best trial point is chosen from the whole mesh. The NOMAD optimizer uses different strategies like Variable Neighborhood Search (VNS) or Latin-Hypercube sampling (LH). During the poll step several trial points around the current optimum are generated on the grid inside of the borders of the poll size parameter  $\Delta_k^p$  (see Fig. 4). The trial points are then passed to the black box program. Once a better result is found, the center of trial points is moved to the new optimum and the mesh size of the grid  $\Delta_k^m$  is enlarged. If no new optimum can be found the mesh size is decreased. The optimization is finished when the maximum number of steps or the minimal mesh size is reached.

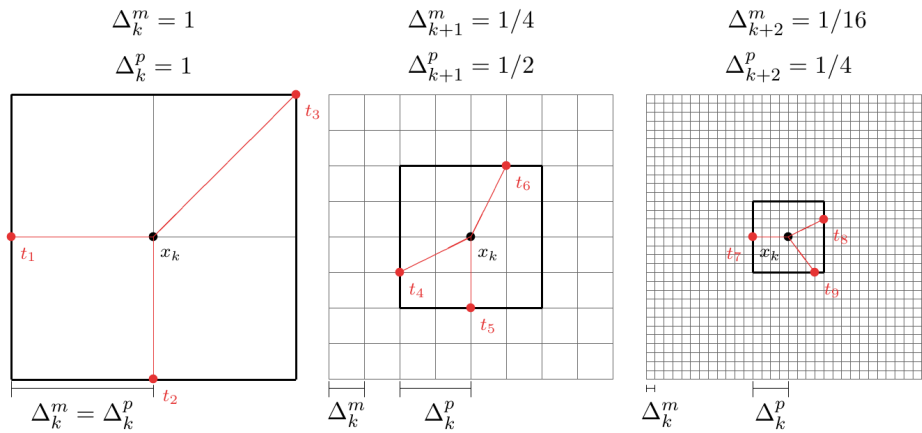


Figure 4: Exemplary mesh configurations [7].

During the poll steps the central trial point can end in a local minima if the poll size became too small. Therefore the metaheuristic strategies VNS and LH are used during the search step. While the LH method just tries to find a better result at random places in the mesh, the VNS method is based on a source of disturbance.

At the end of each run of the burn-off simulator the assessment function  $o_{bj}$  is used to determine the difference between the desired and the calculated thrust curve ( $F_{d,i}$  and respectively  $F_{c,i}$ ) [5].

$$o_{bj} = \frac{1}{F_{d,avg}} \left[ \frac{1}{M} \sum_{i=1}^M |A(F_{d,i} - F_{c,i})|^E \right] \quad (9)$$

The function uses the arithmetic average of the desired thrust  $F_{avg}^d$  and the difference of the thrust at every time step  $i$  ( $M$  is the total number of time steps). The multiplier  $A$  and the exponent  $E$  define how much influence a difference has. Typically the least square method ( $L_2$  norm) is used which implies  $A = 1$  and  $E = 2$ .

In addition a penalty function  $o_{p,time}$  is used to diminish differences in the total burning time ( $t_{c,max}$  and  $t_{d,max}$ ) [5].

$$o_{p,time} = \sqrt{\frac{10^{-3}}{o_{time}}} (t_{c,max} - t_{d,max}) \quad (10)$$

The user can choose the value of  $o_{time}$  to adjust the importance of a time difference. A typical value is  $o_{time} = 0.01$ . NOMAD uses  $o_{bj}$  as assessment function and  $o_{time}$  as constraint.

#### 4. Design of an exemplary booster stage

A propellant grain for a booster stage was designed to test the combination of the burn-off simulation program and the NOMAD optimizer. Most of the input parameters were derived from an earlier proposed rocket motor for the Ariane 6, which has a propellant mass of 120t [2,3,4]. Other parameters were calculated with the CEA code (Chemical

Equilibrium with Applications) [8]. The desired thrust curve (see Fig. 5) has a typical progress for a booster stage consisting of the five characteristic phases [4]. In the first 40 s the maximum thrust of 4 000 kN is reached. After that a plateau with an average thrust of 2 500 kN follows and the burn ends after 125 s with a total impulse of 319 570.5 kNs.

Table 1: Input parameters for the 120t solid rocket motor.

Parameter	Value
Propellant	HTPB1912
Desired thrust curve	see Fig. 5
Total impulse $I_{\text{tot}}$ [kNs]	319 570.5
Specific impulse $I_{\text{sp}}$ [ $\text{ms}^{-1}$ ]	2 737
Maximum chamber pressure $p_{\text{max}}$ [bar]	100
Density $\rho$ [ $\text{kgm}^{-3}$ ]	1 802
Regression rate $\dot{r}$ @ 100 bar [ $\text{mms}^{-1}$ ]	10.16 <sup>a</sup>
Heat capacity ratio $\kappa$ [-]	1.1283
Chamber temperature $T_C$ [K]	3 569
Nozzle expansion ratio $\varepsilon$ [-]	17
Nozzle throat diameter $d_t$ [cm]	54.79

<sup>a</sup> based on the law of St. Robert  $\dot{r} = a \cdot p^n$

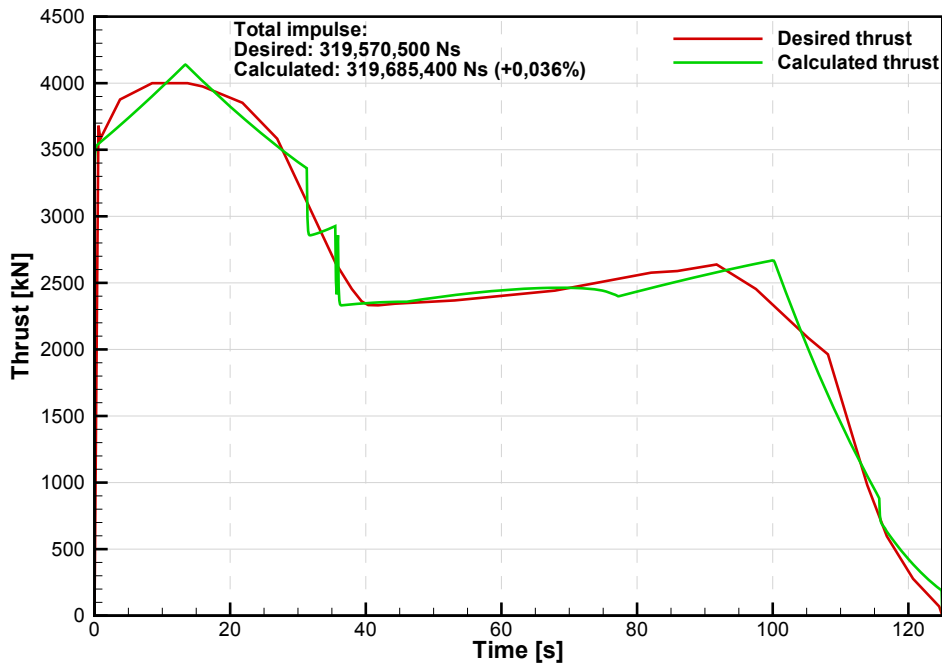


Figure 5: Desired and calculated thrust curve.

The input parameters above are fixed, while most of the parameters in Table 2 are altered by the optimizer. Since the optimizer tries several combinations of the input parameters, seven checks were implemented in the burn-off simulator to prevent results, which are not possible or constructible.

- fin length  $l > 0$ : The fin length  $l$  has to be greater than 0 m.
- inner radius  $r > 0$ : The inner radius  $r$  has to be greater than 0 m.
- $f / \sin(\pi/N) < r$ : When the fin radius  $f$  is too large for the given fin number  $N$  an impossible finocyl geometry is the result.
- $W > (w + f)$ : The maximum web thickness  $W$  must be larger than the sum of the minimum web thickness  $w$  and fin radius  $f$ .
- $r > R/10$ : The inner radius  $r$  of the finocyl geometry has to be at least 10% of the chamber radius  $R$  to prevent a blockage of the flow channel.

- $r_i < R$ : The radii in the cylindrical part of the propellant grain must not be larger than the chamber radius  $R$ .
- $r_7 < (R - w)$ : The radius before the finocyl part  $r_7$  has to be smaller than the radius of the minimum web thickness  $R - w$ .

The ranges of the input parameters were chosen based on experiences of previous motor developments. In addition the upper bound of chamber radius is limited by the capability of the Guiana Propellant Plant in Kourou. The maximum possible chamber diameter is 3.7 m [4]. Also some parameters were fixed or dependent during the optimization. Finally, the optimizer had to solve the resulting 13-dimensional problem. The optimizer was allowed to run 2.5 million evaluations in total.

#### 4.1 Results

Without preparation and post-processing procedures all evaluations took a wall clock time of approximately 72 hours. All calculations were conducted on a local cluster system with 48 cores in parallel. The results are displayed in Table 2 and in Fig. 5. The total impulse of the calculated thrust curve is 319 685.4 kNs, which is 0.036 % accurate. At about 13.3 s the maximum thrust of 4 137 kN is reached.

Table 2: Parameter ranges and results of the optimizer.

Parameter	Lower bound	Upper bound	Result
Chamber radius $R$ [m]	1.0	1.85	1.55712484
Minimum web thickness $w$ [m]	0.05	1.0	0.355409183
Maximum web thickness $W$ [m]	0.2	1.3	1.0453371
Fin radius $f$ [m]	0.02	0.5	0.08613721
Number of fins $N$ [-]	4	25	9
Radius 1, Radius 2 $r_1 = r_2$ [m]	0.2	0.5	0.5
Radius 3, Radius 4 $r_3 = r_4$ [m]	0.2	0.3	0.2
Radius 5, Radius 6 $r_5 = r_6$ [m]	0.3	0.7	0.4507302
Radius 7 $r_7$ [m]	0.3	1.5	0.642005
Radius 10 $r_{10}$ [m] <sup>a</sup>		0.6	0.6
Radius 11 $r_{11}$ [m] <sup>a</sup>		0.8	0.8
Radius 12 $r_{12}$ [m] <sup>a</sup>		0.95	0.95
Length 1 $\Delta L_1$ [m] <sup>a</sup>		0.1	0.1
Length 2 $\Delta L_2$ [m] <sup>a</sup>		0.1	0.1
Length 3 $\Delta L_3$ [m]	0.3	0.6	0.442191
Length 4 $\Delta L_4$ [m] <sup>a</sup>		0.1	0.1
Length 5 $\Delta L_5$ [m]	1.0	8.0	1.0818098
Length 6 $\Delta L_6$ [m]	0.5	0.7	5.4155955
Length 7 $\Delta L_7$ [m] <sup>a</sup>		0.4	0.4
Length 8 $\Delta L_8$ [m]	0.5	5.0	0.6479925
Length 9 $\Delta L_9$ [m] <sup>a</sup>		0.4	0.4
Length 10 $\Delta L_{10}$ [m] <sup>a</sup>		0.2	0.2
Length 11 $\Delta L_{11}$ [m] <sup>a</sup>		0.6	0.6

<sup>a</sup> Fixed value

In Fig. 6 the calculated propellant grain is shown. There is a constriction at the upper end, where the igniter will be placed. Next a short cylindrical part is followed by a slightly opening cone. Then the finocyl geometry is inserted. At the lower end of the grain space was reserved to incorporate the nozzle of the motor.

The overall length of the propellant grain is 9.488 m with a chamber diameter of 3.114 m. The finocyl geometry consists of 9 fins with a fin radius 8.6 cm. With a propellant volume of 59.6 m<sup>3</sup> the total mass results to 107 492 kg. It is planned that monolithic propellant grains with a mass of up to 180 t will be manufactured in the future Guiana Propellant Plant in Kourou [2, 10]. Therefore, the here proposed motor will be casted in one step. The overall geometry is beneficial for an easy manufacturing process.

## 5. Conclusions

In this paper a common propellant grain geometry of a solid rocket motor with a cylindrical and a finocyl part was described. The finocyl geometry is defined by five parameters. During the burn-off the burning area can be calculated

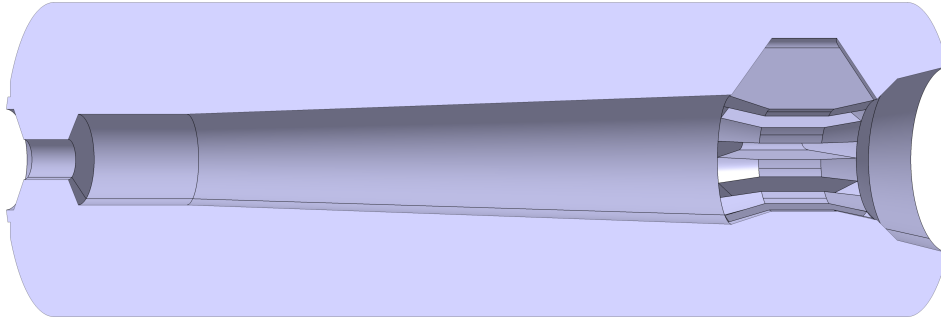


Figure 6: Calculated propellant grain.

via the above described perimeter equations. The cylindrical part of the grain consists of 11 cylindrical and conic parts, which are described by 12 coordinate tuples. The surface areas during the burn-off of both parts can be determined with a sufficient accuracy.

To find the grain geometry fitting to the required thrust curve, the optimizer NOMAD was applied. NOMAD uses the MADS algorithm with the help of the metaheuristic VNS and LH methods. The optimization is conducted based on an assessment function, which is calculated by the least square method of the thrust difference between the desired and the calculated thrust curve. An additional constraint ensures that there is no difference in burning time.

The combination of the burn-off simulator and the optimizer was tested with the design of a booster stage. A typical thrust curve was used as optimization target. The input parameters were derived from an earlier investigated booster stage for the Ariane 6. NOMAD then had to find an optimal solution inside a 13-dimensional problem within the given ranges. To avoid impossible solutions several checks were defined and explained. In total 2.5 million evaluations were conducted within a short period of time. The resulting differences between the calculated and the desired thrust curve are only marginal (0.036%). Furthermore the geometry of the propellant grain can be casted at the future propellant plant in Kourou.

The optimization of finocyl grain geometries using a black box optimizer and a burn-off simulation tool can accelerate the design process of solid rocket engines and it is sufficiently accurate. The next steps are the implementation of rounding edges and a better description of the transition zones between the cylindrical and finocyl parts of the propellant grain. However a consistent predesign of a propellant grain is already possible.

## References

- [1] Abramson, M.A. et al.: The NOMAD project. Software available at <http://www.gerad.ca/nomad>.
- [2] Boury, D. et al.: Large Solid Rocket Motors for Future European Launcher. AIAA 2012-3888. In *48<sup>th</sup> AIAA/ASME/SAE/ASEE Joint Propulsion Conference & Exhibit*, Atlanta, GA, 2012.
- [3] Dumont, E. et al.: Advanced TSTO launch vehicles. In *4<sup>th</sup> European Conference for Aerospace Sciences (EU-CASS)*, St. Petersburg, 2011.
- [4] Dumont, E.: Variations of Solid Rocket Motor Preliminary Design for Small TSTO launcher. In *Space Propulsion 2012*, Bordeaux, 2012.
- [5] Johansson, M.: Optimization of Solid Rocket Grain Geometries. Master thesis, *KTH Royal Institute of Technology*, Stockholm, 2012.
- [6] Koch, P.: Optimization of Solid Grain Geometries for Hybrid and Solid Rocket Engines. Master thesis, *Technische Universität Braunschweig*, 2014.
- [7] Le Digabel, S.: Algorithm 909: NOMAD: Nonlinear Optimization with the MADS algorithm. *ACM Transactions on Mathematical Software*, 37(4):44:1-44:15, 2011.
- [8] McBride, B. J. and Gordon, S.: Computer Program for Calculation of Complex Chemical Equilibrium Compositions and Applications - II. Users Manual and Program Description. *National Aeronautics and Space Administration, Lewis Research Center*, Cleveland, OH, 1996.
- [9] Rajesh, K. K., Anantharam, S. and Subhash Chandran, B. S.: Analytical Expressions for Burning Perimeter and Port Area for a Solid Propellant Finocyl Grain. AIAA 2007-5784. In *43<sup>rd</sup> AIAA/ASME/SAE/ASEE Joint Propulsion Conference & Exhibit*, Cincinnati, OH, 2007.
- [10] Saint Martin, S. et al.: Twin Screw Process Demonstration Technology Activities for Solid Propulsion in New Generation Launcher Applications. In *63<sup>rd</sup> International Astronautical Congress (IAC)*, Naples, 2012.